SEDIMENTOLOGY the journal of the International Association of Sedimentologists

Sedimentology (2010) **57,** 845–856 doi: 10.1111/j.1365-3091.2009.01122.x

Architecture of an Oligocene fluvial ribbon sandstone in the Ebro Basin, North-eastern Spain

GUSTAVO GONZÁLEZ-BONORINO*, FERNANDO COLOMBO† and LILIANA ABASCAL‡
**Centro Austral de Investigaciones Científicas (CADIC-CONICET), Bernardo Houssay 200, 9410 Ushuaia, Argentina (E-mail: bonorino@cadic.gov.ar)*
†Dept. Estratigrafia, Paleontologia i Geociències Marines, Fac. Geologia, Universitat de Barcelona, Martí i Franquès, s/n, E-08028 Barcelona, Spain
‡Facultad Regional Río Grande, Universidad Tecnológica Nacional, 9420 Río Grande, Tierra del Fuego, Argentina

ABSTRACT

Fluvial ribbon sandstone bodies are ubiquitous in the Ebro Basin in North-eastern Spain; their internal organization and the mechanics of deposition are as yet insufficiently known. A quarrying operation in an Oligocene fluvial ribbon sandstone body in the southern Ebro Basin allowed for a three-dimensional reconstruction of the sedimentary architecture of the deposit. The sandstone is largely a medium-grained to coarse-grained, moderately sorted lithic arenite. In cross-section, the sandstone body is 7 m thick, occupies a 5 m deep incision and wedges out laterally, forming a 'wing' that intercalates with horizontal floodplain deposits in the overbank region. Three architectural units were distinguished. The lowest and highest units (Units A and C) mostly consist of medium-grained to coarse-grained sandstone with medium-scale trough cross-bedding and large-scale inclined stratasets. Each of Units A and C comprises a fining-up stratal sequence reflecting deposition during one flood event. The middle unit (Unit B) consists of thinly bedded, fine-grained sandstone/mudstone couplets and represents a time period when the channel was occupied by low-discharge flows. The adjoining 'wing' consists of fine-grained sandstone beds, with mudstone interlayers, correlative to strata in Units A and C in the main body of the ribbon sandstone. In plan view, the ribbon sandstone comprises an upstream bend and a downstream straight reach. In the upstream bend, large-scale inclined stratasets up to 3 m in thickness represent four bank-attached lateral channel bars, two in each of Units A and C. The lateral bars migrated downflow and did not develop into point bars. In the straight downstream reach, a tabular cross-set in Unit A represents a mid-channel transverse bar. In Unit C, a very coarse-grained, unstratified interval is interpreted as deposited in a riffle zone, and gives way downstream to a large mid-channel bar. The relatively simple architecture of these bars suggests that they developed as unit bars. Channel margin-derived slump blocks cover the upper bar. The youngest deposit is fine-grained sandstone and mudstone that accumulated immediately before avulsion and channel abandonment. Deposition of the studied sandstone body reflects transport-limited sediment discharges, possibly attaining transient hyperconcentrated conditions.

Keywords Ebro Basin, fluvial, Oligocene, ribbon sandstone, Spain.

INTRODUCTION

Oligocene strata in the southern Ebro Basin, North-eastern Spain (Fig. 1), comprise numerous narrow and elongate (width/depth < 15/1) fluvial sandstone bodies that fill channels incised into floodplain strata (Riba *et al.*, 1967). Williams (1975) and Friend *et al.* (1979) applied the term ribbon sandstone to these deposits. In cross-section, sandstone bodies commonly show a maximum thicknesses from 1 to 7 m in central parts and wedge out laterally and up the bank slope, forming 'wings' that extend beyond the channel into the floodplain area (Friend *et al.*, 1979; Allen *et al.*, 1983). The thickness of any sandstone body is usually slightly greater than the depth of the scour ('superelevation' of Möhrig *et al.*, 2000). Internally, many of these bodies show large-scale inclined bedsets (nomenclature of Bridge, 2006) and trough cross-bedded sets, commonly organized into storeys bounded by stratal discontinuities (Friend *et al.*, 1979; Allen *et al.*, 1983; Möhrig *et al.*, 2000). The large-scale inclined stratasets have been interpreted as freely migrating channel bar deposits (Möhrig *et al.*, 2000) and 'downstream accretion macroforms' (Cuevas *et al.*, 2007). More generally, the sandstone bodies have been attributed to ephemeral stream environments on a distal alluvial plain (Friend *et al.*, 1979; Allen *et al.*, 1983; Cuevas *et al.*, 2007).

Fluvial ribbon sandstone bodies in the southern Ebro Basin share important likenesses in geometry and sedimentary structures to analogous bodies in northern parts of the Ebro Basin (e.g. Nichols, 2007) as well as in other basins (e.g. Stear, 1983; Smith, 1995; Gibling & Rust, 2006; King, 2008), suggesting common genetic features. The widespread distribution of fluvial ribbon sandstones and their potential as hydrocarbon reservoirs (Bridge *et al.*, 2000) warrant a better understanding of the fluvial processes involved in their development. The Ebro Basin offers an exceptional opportunity for such studies.

Most published descriptions of the Ebro Basin ribbon sandstone bodies are piecemeal and two-dimensional (e.g. Cabrera *et al.*, 1985; Anadón *et al.*, 1992; Cuevas *et al.*, 2007), and are insufficient to reconstruct adequately their sedimentary architecture and infer the processes associated with bar formation and migration, and channel incision and infilling. An active quarry located in the southern Ebro Basin allowed a detailed, three-dimensional description of one ribbon sandstone body over 100 m in length, and the documentation of the spatial arrangement of lithofacies and elucidation of the fluvial mechanics involved in its development. It is concluded here that 80% of the sandstone body accumulated during only two major flood events, and that much of the sediment was deposited as mid-channel and lateral bars that migrated during high flow stages but were not associated with significant channel widening or displacement through lateral erosion. High sedimentation rates and vertical aggradation of the river bed characterized the channel fluvial

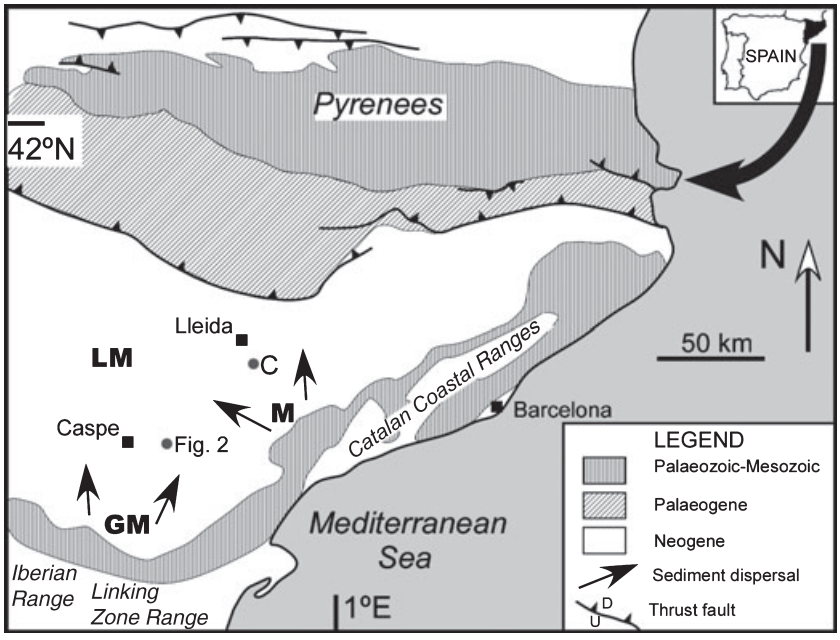

Fig. 1. Simplified geological map of the Ebro Basin. Sediment dispersal patterns are shown schematically by arrows for the Oligocene upper Montsant 'M' and the Guadalope–Matarranya 'GM' alluvial fan/channels depositional systems; 'LM' – evaporitic Los Monegros Basin; 'C' – approximate position of study area in Cantacorbs quarry.

regime. Favoured by outstanding exposures, the reconstruction presented herein will serve as a working model against which to compare less-extensive exposures in the Ebro Basin and elsewhere and eventually establish the range of variation in architectural characteristics of these bodies.

PALAEOGEOGRAPHIC SETTING

The Ebro sedimentary basin, in North-eastern Spain, is bounded by the Pyrenees to the north, and by the Iberian, Linking Zone, and Catalan Coastal Ranges along the south (Fig. 1; review in Santanach, 1997). In the Oligocene, the fluvial–alluvial Guadalope–Matarranya and the slightly older Montsant depositional systems flowed northward from these ranges across the southern Ebro Basin, finally merging with Los Monegros evaporitic and lacustrine environments in central parts of the endorheic basin (Fig. 1; Cabrera *et al.*, 1985; Anadón *et al.*, 1989; Villena *et al.*, 1992; Swanson-Hysell, 2005). Mammal remains, fossil flora and the evaporitic deposits indicate that Oligocene climate in the Ebro Basin area was arid to semi-arid (Williams, 1975; Cabrera *et al.*, 1985; Barbera *et al.*, 2001).

Ribbon sandstone bodies are most numerous in the Caspe Formation of the Guadalope–Matarranya System (see Möhrig *et al.*, 2000; for a partial aerial view of these exposures) but are also present in the upper Montsant System. Between 1991 and 2001, the Cantacorbs quarry, located near the city of Lleida (Fig. 1), progressively exposed one ribbon sandstone body in the upper Montsant System. For the present study, the quarry was surveyed in July 1994, May and August 1996, February and September 1998, July 1999, November 2001 and December 2002. The quarry faces were mapped and photographed, and detailed features were recorded as quarrying progressed. The exposed length of the sandstone body is 105 m. Almost 400 m of quarry faces, up to 7 m high, with over 90% of exposure were surveyed. In 1994, much of the south-western margin of the sandstone body and channel had been eliminated and was not available for inspection (Fig. 2).

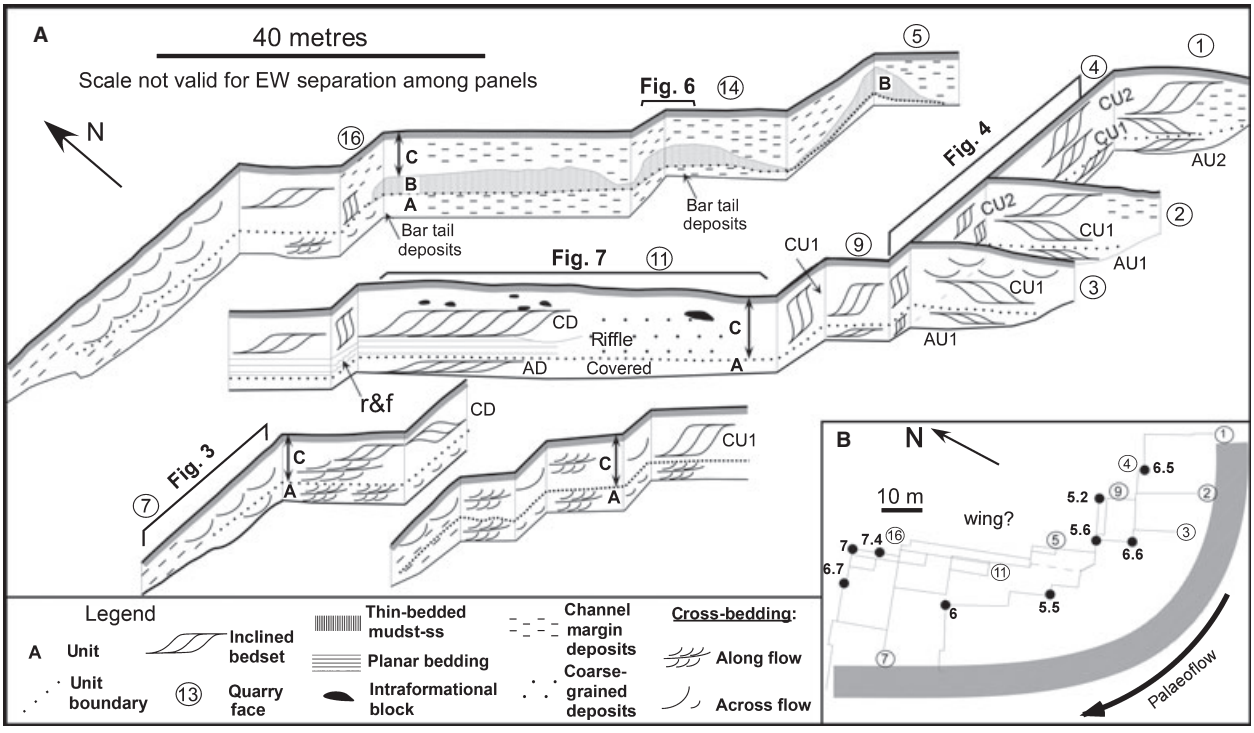

Fig. 2. (A) Schematic view of the fluvial architecture of the Cantacorbs sandstone body based on photographic panels of quarry faces. For clarity, the scale in an east–west direction is slightly exaggerated and the vertical scale is 200%. 'r&f' – ridge and furrow morphology mentioned in the text. (B) Inset shows the progressive position of quarry faces. Wing deposits adjoining the left-hand channel margin are indicated by a diagonally ruled grey band. The thickness of the channel fill is given for positions at solid circles. In both drawings, circled numbers indicate quarry faces mentioned in the text. [mudst-ss = mudstone-sandstone]

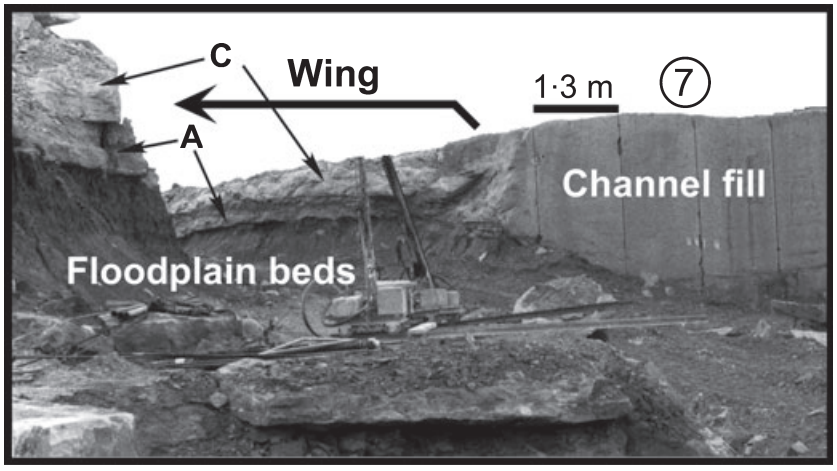

Fig. 3. Cross-section of a sandstone body perpendicular to the channel direction near the downstream end of the exposure. The crane rests on sandstone intercalated in the floodplain strata. Wing deposits crop out in the left half of the photograph. The arbitrary boundary between wing deposits and the channel-fill at the uppermost break in slope is indicated by a half bracket. Units A and C are represented in the wing by correlative strata of fine-grained sandstone and mudstone. The circled number indicates a quarry face in Fig. 2.

THE RIBBON SANDSTONE BODY

The studied sandstone body reaches a maximum thickness of 7·4 m along the axis of the channel, and a width of *ca* 40 m. One wing was exposed, extending into the left overbank region (looking downflow; Fig. 2B) where it is intercalated with floodplain deposits represented by horizontally laminated, reddish to purplish mudstone that alternates with greenish, thin-bedded, rippled and horizontally laminated sandstone units. The channel-fill is arbitrarily separated from the wings at the uppermost break in the slope of the incision (Fig. 3). The base of the sandstone body is a 5 m deep erosion surface carved into floodplain strata, whereas its upper surface consists of irregular ridges and swales with local relief of up to 1 m; mudstone layers are preserved in some of the swales. Compositionally the sandstone is a medium to coarse-grained, moderately sorted lithic arenite with more than 90% of the framework grains consisting of limestone fragments derived from the Mesozoic to lower Tertiary cover in the Catalan Coastal Ranges (Colombo, 1994). Local palaeoflow direction was from south-east to north-west (Fig. 2B), in agreement with interpretations by Allen *et al.* (1983) from nearby exposures. The Cantacorbs quarry exposures represent fluvial bar and channel fill deposits comprising a curved reach upstream and a straight reach downstream.

Architectural units

Two erosion surfaces, internal to the sandstone body, allow for the distinction of Unit A (below), Unit B (middle) and Unit C (top) (Figs 3 to 5).

Unit A

Unit A varies in thickness from < 0·4 m to more than 1·5 m, and makes up *ca* 25% of the channel fill volume. It constitutes a fining-upward succession in which local lag deposits at its base are overlain by medium-grained and coarse-grained sandstones, which, in turn, are overlain by fine-grained sandstones with mudstone partings at the top.

The basal lag deposits are of two types: (i) lenses of mudstone breccia with intraformational fragments ranging in size from granules to cobbles; and (ii) structureless layers of coarse-grained sandstone. Basal lag deposits mantle the lower third of flank slopes in both the upstream and the downstream reaches (Figs 2, 4, 5A and 5B). The lag deposits probably accumulated shortly below the level of maximum near-bank flow velocity. In the upstream reach, Unit A includes two partly overlapping, large-scale (*ca* 1·5 m thick) inclined bedsets interpreted as representing parts of channel bars AU1 (below) and AU2 (above) (AU from Unit A Upstream reach; Figs 4 and 5B). Bar AU1 accreted downstream and towards the left bank (looking downflow; Fig. 5B), whereas bar AU2 accreted downstream and towards the right bank. Bar AU2 was well-exposed only at quarry face 1 (Fig. 2A), where it overlaps the thin (< 0·5 m thick) upstream slope deposit of bar AU1. Bar AU1 was exposed more completely in quarry faces 1, 2, 3 and 4 (Fig. 2). It comprises a large (1·4 m thick, 30 m in exposed downstream length and *ca* 15 m wide) sigmoidal strataset with dips of 12 to 15° and a topset to bottomset relief of *ca* 1 m (Fig. 5B). Within the inclined beds, trough cross-sets 0·05 to 0·1 m thick indicate dune migration obliquely down the bar front and

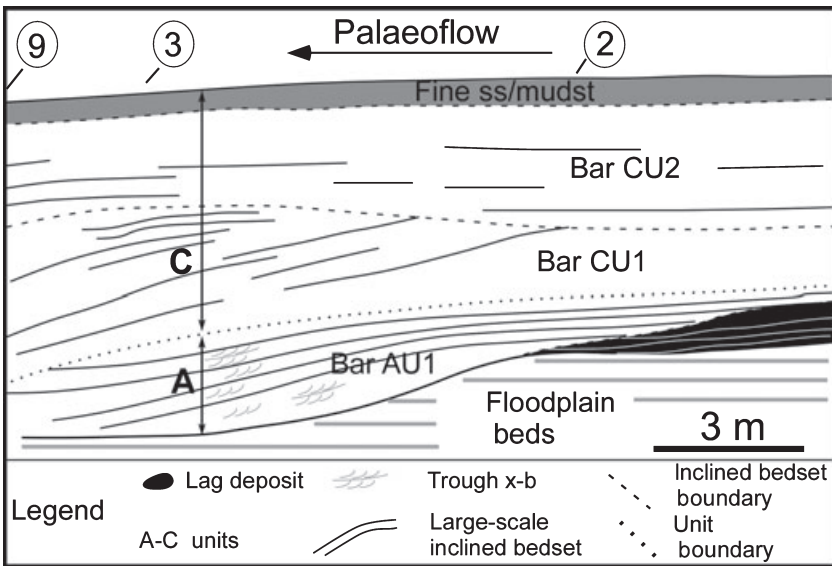

Fig. 4. Cross-section along the upstream reach between quarry faces 1 and 9 (quarry face 4 in Figs 2 and 5B; flow towards the left). Note the topset accretion in bars AU1 and CU2. Inclined bedsets in bar AU1 show small-scale trough cross-bedding (x-b) and pass into horizontal bottomsets. Inclined bedsets in bar CU2 dip away from the viewer and downstream. The circled numbers indicate intersections with quarry faces 2, 3 and 9. No vertical exaggeration. [ss/mudst = sandstone/mudstone]

towards the right bank (Fig. 4). Fine-grained sandstone with mudstone partings makes up the uppermost topsets in bar AU1 and indicates waning flow over the bar top (Fig. 5B); one semi-circular scour (0·5 m wide and 0·2 m deep) into the lower slope of the bar may represent a cross-over channel (Fig. 5B). The downstream termination of bar AU1 lies within the bend.

Up the slope of the right margin, topsets gradually give way to fine-grained sandstone, in places thinly bedded with mudstone partings; a facies herein designated channel margin facies. These deposits resemble those in Unit B. Channel margin strata mantle the slopes of the incision and merge with the wing deposits (Fig. 5B).

In the straight downstream reach, along the palaeochannel thalweg, the basal part of Unit A (an estimated 0·3 m thickness) generally was not exposed because it lay below the quarry floor. In this sector, the exposed base of Unit A partly consists of medium-grained sandstone forming a tabular cross-set *ca* 0·8 m in thickness and *ca* 20 m in length in the downflow direction, with foresets dipping 16° parallel to palaeoflow (bar AD, from Unit A Downstream reach; Fig. 5A), and capped by topsets of fine-grained sandstone with wavy bedding making up the horizontal bar top. Adjacent to the right bank, distal facies of bars AD and AU1 show fine-grained silty sandstones that locally show climbing ripples, convolute lamination and one medium-scale cross-set (0·4 m thick) accreting against the dominant river flow direction. These beds (Fig. 6), lying at the base of Unit A, are interpreted as marginal bar tail deposits.

Unit B

Unit B measures up to *ca* 2·5 m in thickness and accounts for < 5% of the ribbon sandstone volume. It rests with sharp angular discordance on Unit A marginal bar tail deposits adjoining the right bank (Figs 5A and 6). Unit B comprises thin beds of fine-grained, ripple cross-laminated sandstone alternating with moderately bioturbated mudstone, features that suggest deposition from low-discharge flows and from ponded water on the channel bottom. It is presumed that a large portion of Unit B in central parts of the channel was eroded away previous to the deposition of Unit C.

Unit C

Unit C overlies a scour with a 3·5 m relief that cuts through Unit B, reaching deeply into Unit A (Fig. 5). Unit C varies in thickness from 1 to 5·8 m and makes up *ca* 70% of the sandstone body volume. Unit C constitutes a fining-upward sequence with isolated lenses of mudstone breccia at the base, followed by coarse-grained, planar-bedded sandstone and medium-grained and coarse-grained sandstone with large-scale inclined bedding, and capped by fine-grained sandstone and mudstone.

In the upstream reach, Unit C comprises two partly overlapping, large-scale (1·8 to 3 m in thickness, *ca* 30 m in length downstream and 10 to 15 m in width), inclined stratasets that accrete downflow and towards the left bank (the lower bar CU1) and the right bank (the upper bar CU2), with topset to bottomset relief of *ca* 1·5 m (Fig. 5B). Bars CU1 and CU2 show similar lateral

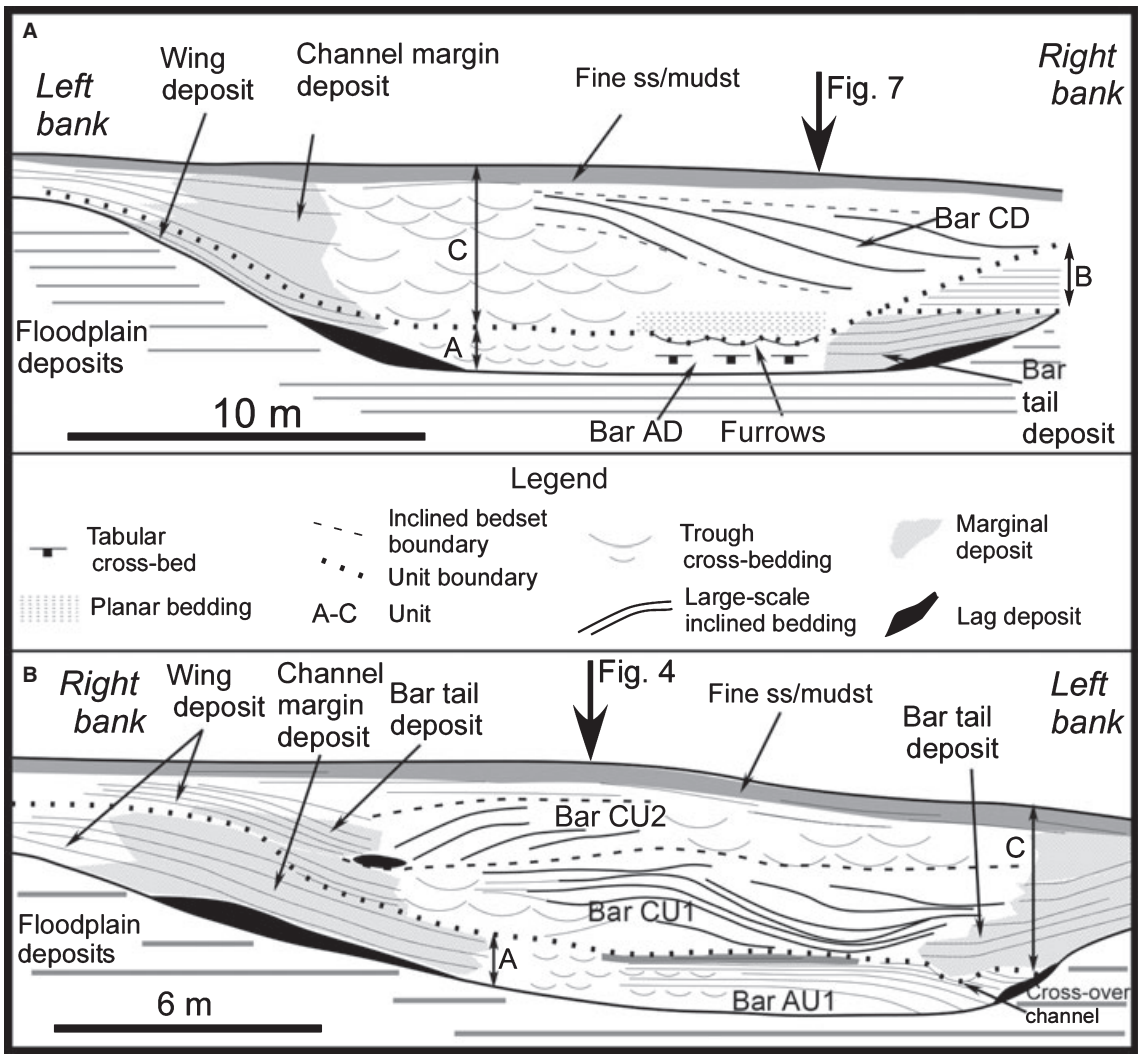

Fig. 5. Cross-sections perpendicular to the trend of the ribbon sandstone body. (A) Composite section extending between quarry faces 7 and 16 in the downstream reach. Unit B beds overlie a narrow erosive terrace against the right channel margin. Flow is away from the viewer. The intersection with Fig. 7 is shown. (B) Composite section of quarry faces 5 and 2 in the upstream reach. The thick grey line at the top of bar AU1 indicates fine-grained sandstone with mudstone partings. Flow is towards the viewer. The intersection with Fig. 4 is shown. [ss/mudst = sandstone/mudstone]

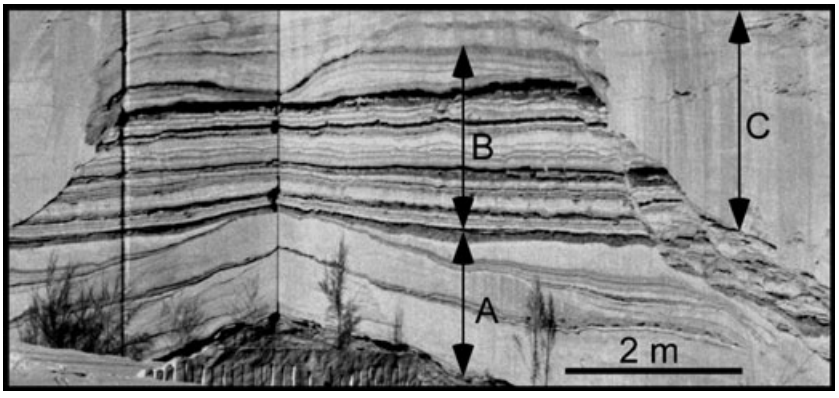

Fig. 6. Unit B horizontal strata, with a local slump block, unconformably overlies Unit A fine-grained sandstone beds with mudstone partings attributed to bar AU1 tail deposits, and are overlain by Unit C channel margin deposits. See Fig. 2A for location.

facies successions across-flow, from channel margin deposits, to trough cross-bedded sandstone with trough cross-sets 0·3 m thick and 2 to 3 m wide across flow, to inclined bedding, and, finally, to concave-up bottomsets and structureless sandstone beds adjacent to the opposite bank (Fig. 5B). In a cross-section along flow (quarry face 4 in Fig. 2), bedding in bar CU2 truncates inclined bedsets in bar CU1 (Fig. 4), indicating bedform translation and erosion over the leeside of bar CU1. Bar CU2 wedges out downflow at about quarry face 9 (Fig. 2A).

In the straight downstream reach, Unit C shows marked architectural changes across-flow (quarry face 11 in Fig. 2). In the upstream half of the reach the lower half of Unit C is dominated by unstratified, and apparently structureless, medium-grained sandstone with numerous pebble-size to boulder-size intraformational lithic fragments (Fig. 7). Downflow, this interval gives way to two distinct stratasets. In the lower part of Unit C, overlying basal lenses of mudstone breccia are beds of planar-bedded, coarsely laminated, coarse-grained sandstone that show a ridge and furrow morphology in across-channel sections (position indicated as 'r&f' in Fig. 2A). This lithofacies is interpreted as deposited under washed-out dunes to upper flow regime plane-bed conditions, with the ridges and furrows formed by large-scale horizontal vortices parallel to the main water flow. Similar bedforms have been described by Coleman (1969) from the Brahmaputra River, and Wilson (1973) postulated that longitudinal paired vortices may commonly develop in straight river reaches.

Above the planar bedding interval a large-scale, sigmoidal sandstone strataset measuring 1 to 3 m in thickness, >30 m in length downstream and >15 m in width, represents bar CD (Figs 5A and 7); inclined beds from this bar downlap onto eroded Units A and B underlying the right bank (Fig. 5A). The large-scale strataset thins westward, away from the thalweg, merging with tabular cross-beds underlying a 10 to 15 m wide sandstone platform that separates the inclined bedset from the channel margin deposits attached to the left flank of the incision (Fig. 5A). Minor erosion surfaces delimit three subsets (designated as '1', '2' and '3' in Fig. 7); the lowest subset rests unconformably on concave-up strata (Fig. 7).

A well-defined interval of intraformational breccia, with fragments measuring up to 3 m in length in a matrix of smaller mudstone fragments and sandstone, extends along most of the downstream reach, overlying the very coarse-grained deposits and the inclined bedset in bar CD. The lithology of the blocks resembles that of the channel margin deposits rather than the muddy, thin-bedded floodplain strata. The block furthest downstream appears to be partly buried by inclined strata in the more recent subset ('1' in Fig. 7), suggesting that late-stage development of bar CD was partly contemporaneous with slumping.

The uppermost 0·1 to 1·0 m in Unit C consists of fine-grained sandstone and mudstone, with inconspicuous bedding, which makes up *ca* 5% of the sandstone body thickness (indicated by a grey band at the top of Unit C in Fig. 2). Its base is ill-defined and its top is the top of the sandstone body. This bed marks the end of sedimentation of the Cantacorbs ribbon sandstone.

Wing deposits

The wings of the sandstone body comprise thinly bedded, laminated, fine-grained sandstone

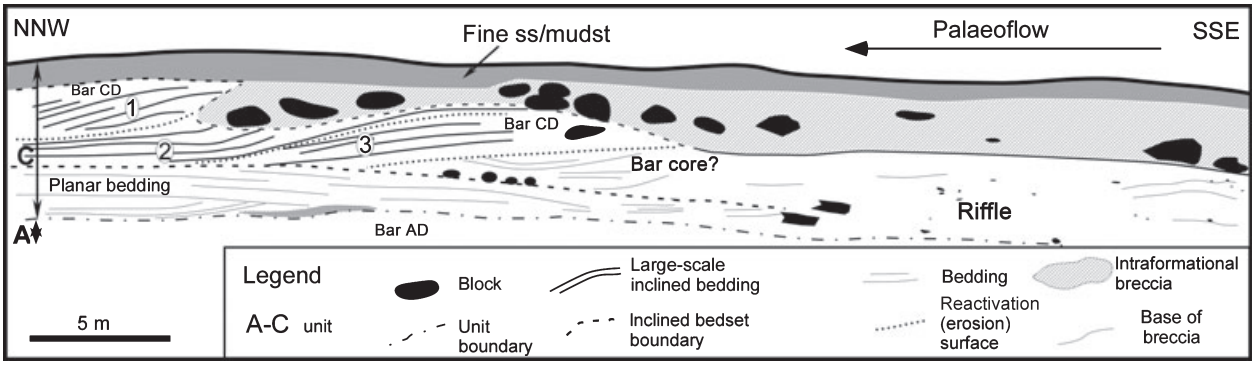

Fig. 7. Bedding in Unit C along the downstream reach (quarry face 11 in Fig. 2). In the lower third, Unit C shows plane-laminated sandstone; above follows the large-scale inclined stratasets of bar CD, with minor erosion surfaces delimiting subsets '1', '2' and '3'. Large intraformational fragments (in black) rest on the bar strataset; only the larger blocks are indicated. No vertical exaggeration. See Figs 2 and 5A for location. [ss/mudst = sandstone/mudstone]

beds with mudstone partings, deposited on top-bank and overbank locations. Lateral fining takes place over *ca* 2 to 4 m, accompanying rapid thinning of the sandstone body up the bank slope (Fig. 3). Wing strata are laterally equivalent to strata in Units A and C (Figs 3 and 5), indicating deposition largely concurrent with that of the ribbon sandstone. Wing strata do not show intercalations of floodplain beds, suggesting that the time span for wing development was short relative to floodplain rates of sedimentation.

INTERPRETATION AND DISCUSSION

An original bar morphology is inferred for the large-scale inclined stratasets on the basis of: (i) planform dimensions scaled to bankfull channel width; (ii) sigmoidal stratal arrangement; and (iii) superimposed dune cross-bedding. Substantial vertical accretion is inferred from the complete preservation of the topsets. Similarly, partial superposition of bars AU2 on AU1, and CU2 on CU1, suggest vertical accretion of the river bed coupled to downstream or lateral migration of the bars. Vertical accretion would reflect deposition at high rates from a flow at transport-limited sediment load capacity. High sedimentation rates were a characteristic regime in the Cantacorbs channel.

In upstream Unit A, bars AU1 and AU2 developed as lateral bars attached to opposite margins of the incision (Figs 2 and 8A). Bar AU2 originated upstream of the studied reach and extended to quarry face 1, whereas the bulk of bar AU1 lay between quarry faces 1 and 3, approximately. Thus, the bars were not associated strictly with bend development, as would be expected for point bars; rather, they migrated freely downcurrent along the bend. The length of bar AU1 is about twice the palaeoflow width, which is rather short when compared to fully developed alternate bars (cf. Bridge, 2003). This effect may have been due to: (i) insufficient duration of the flow (cf. Tubino, 1991); and (ii) significant storage of sand in vertical accretion deposits at the expense of lengthening. Similarly, bars CU1 and CU2 in upstream Unit C are interpreted as lateral bars (Fig. 8B and C). In both Units A and C, the bars upstream extended downflow, overtaking the downstream bars. Bar CU2, in particular, overlies much of the length of bar CU1 (Fig. 4) and may reflect a stage in the development of a compound bar. The simple architecture of the surveyed lateral bars suggests that they may be unit bars. The concave-up bottomsets and structureless finer-grained sandstone beds on the downflow fringes of the surveyed bars would represent bar-tail environments. The bodies of the lateral bars between the channel margin deposits and the inclined bedsets are made up of medium-scale, trough cross-bedded deposits. Digitation among the trough cross-beds and the inclined stratasets in across-flow sections suggests that the dunes transported sand that fed the inclined bedsets and that the contact between the areas of deposition of each lithofacies fluctuated. The overall facies arrangement may have resembled the reconstruction for Carboniferous lateral bar formation by Haszeldine (1983, fig. 13).

In the downstream reach, in Unit A (Fig. 8A), the tabular cross-bedded bar AD is flat-topped (cf. Smith, 1971), apparently lacks connection to any of the channel margins and has foresets dipping parallel to palaeoflow; using these observations, bar AD is interpreted as a mid-channel transverse bar. Correlative beds against the right bank, showing arrested-flow and reverse-flow depositional structures, may represent the tail of bar AD. In Unit C (Fig. 8B), the very coarse-grained and unstratified deposits at the exit from the bend reflect deposition in a riffle zone. Immediately downflow from the riffle deposits, sandstones with upper flow regime, or near upper flow regime, planar bedding may reflect initial flooding and transient shallow depths (Fig. 8B). Above these beds was deposited the inclined bedset of bar CD (Fig. 8C); the concave-up stratification at its upstream end might represent scoured unit bars forming the nucleus of bar CD. The erosion surfaces separating subsets 1, 2, and 3 in bar CD (Fig. 7) may have formed through the passage of large dunes (cf. Reesink & Bridge, 2007) or fluctuations in the main thread of the current, but show no evidence for association with low-stage flows.

The inclined strataset thickens from west to east, towards the channel thalweg, at the expense of the trough cross-bedded section (Fig. 5A). A similar architecture was reported by Sambrook Smith *et al.* (2006, fig. 5A) from a ground-penetrating radar survey in the South Saskatchewan River, Canada. The thinner western margin of the inclined bedset shows angle-of-repose cross-bedding, perhaps reflecting relatively lower superimposed dunes away from the main thread of the flow (cf. Reesink & Bridge, 2007). The wide expanse of trough cross-bedded sandstone separating the inclined strataset in bar CD from the left

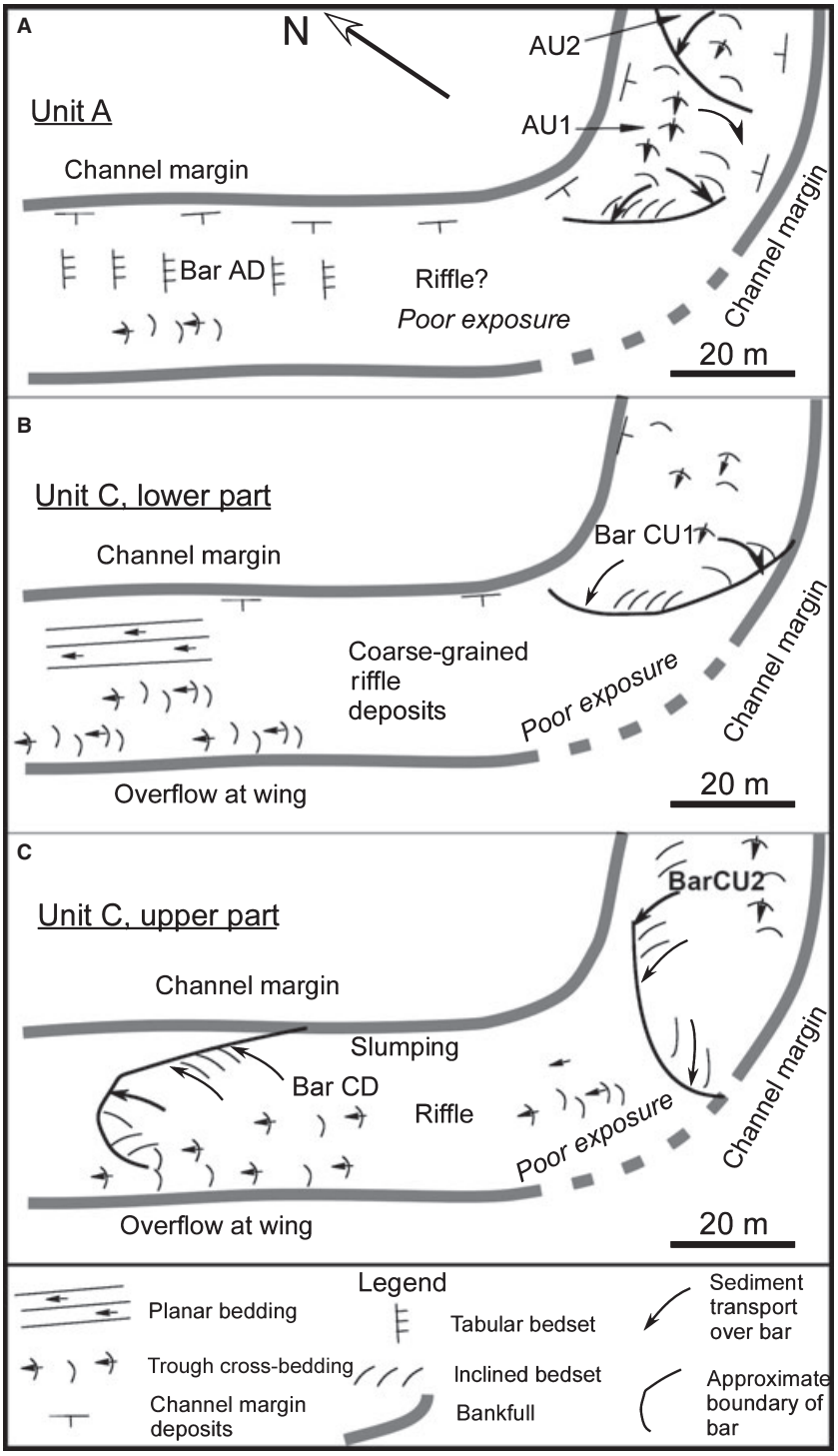

Fig. 8. Schematic plan-view reconstruction of bedform distribution during deposition of: (A) Unit A; (B) lower part of Unit C; and (C) upper part of Unit C. The thick grey lines approximately correspond to the bankfull channel width. Floodplain strata are not represented.

margin of the incision suggests that growth of the bar was detached from the left bank, evolving as a mid-channel macroform (Fig. 8C). Adjacent to the right bank slope, in turn, downlapping distal and finer-grained portions of the inclined CD bedset (Fig. 5A) are interpreted as bar-tail deposits. Overall, bar CD (Fig. 7) shows significant similarities with facies organization in the mid-channel bar in the Jamuna River, Bangladesh, described by Best *et al.* (2003, fig. 9).

Deposition of the inclined bedsets in bar CD appears to have taken place in part contemporaneously with slumping of intraformational blocks into the channel. This is so because, whereas the

majority of the blocks rest on top of the inclined bedset, the block located furthest downstream is partly buried by inclined beds (Fig. 7). Thus, slumping probably occurred during high-stage flow erosion of channel margin deposits on the right flank of the channel. Luppi *et al.* (2009) found that bank failure typically occurs at peak flow.

The fine-grained sandstones making up the channel margin facies, which were deposited above the level of the bar platform, reflect deposition in areas of slower, marginal river flow. These areas appear to have been well-established along the inner – right-hand side – of the upstream bend, and generally over upper slopes of the incision.

Units A and C each constitute a fining-up sequence deposited from an individual flood event. During this stage, two alternate bars developed in the upstream reach, whereas in the straight downstream reach tabular trough cross-sets developed towards the left margin and the transverse bar AD developed closer to the channel thalweg (Fig. 8A). By the end of deposition of Unit A, the Cantacorbs channel had been filled to about one-third of its depth. The fine-grained, rippled and bioturbated beds in Unit B gradually filled much of the remaining channel space. The apparent absence of mud cracks and root marks in these beds would indicate that the channel maintained low-discharge flow and ponded water between flood events. Deposition of Unit C began after deep scouring into Units B and A. During early deposition of Unit C, lateral bar CU1 co-existed with very coarse riffle deposits at the exit from the bend and upper flow regime, or near upper flow regime, plane beds further downstream (Fig. 8B). This stage was followed immediately by the development of lateral bar CU2 upstream and mid-channel bar CD downstream, separated by riffle deposits (Fig. 8C).

Stratal continuity between the wing and the main ribbon sandstone body (cf. Fig. 3), and the apparent absence of crevasses, suggest that the wings were deposited from overbank splays when bankfull conditions, that is, a water depth of *ca* 5 m, were attained both during Unit A and Unit C time. For Unit C time, vertical accretion in the wing areas more or less kept pace with channel bottom elevation (cf. Fig. 5A). The fine-grained bed capping Unit C (grey band in Fig. 2) is interpreted as having accumulated in local depressions from low-discharge flows, shortly before avulsion. During deposition of Unit B beds, on the other hand, flows would have been completely contained in the channel.

The Cantacorbs sandstone body records two major erosional events: initial erosion into floodplain deposits and later erosion into Units A and B prior to deposition of Unit C. Depth of erosion was similar in both cases, *ca* 4 to 5 m, suggesting hydraulic fit between available water discharges and the preserved incision. It is thus possible to speculate that channel incision and infill were consecutive stages in one and the same flooding event (cf. Möhrig *et al.*, 2000), perhaps through mechanisms shown in flume experiments by Sheets *et al.* (2007). The capacity for vertical and lateral erosion and the abundance of dune cross-stratification indicate that flows were fully turbulent. On the other hand, the apparent absence of trough cross-bedding in several of the large-scale inclined bedsets may reflect a transient hyperconcentrated flow condition that would have favoured transition to plane beds (see, for instance, Wan, 1985).

CONCLUSIONS

Study of the Cantacorbs ribbon sandstone body revealed a sedimentary architecture and evidence for fluvial mechanics that had not been documented clearly in previous studies of the Ebro Basin ribbon sandstones. Three architectural units were distinguished on the basis of internal erosion surfaces. Unit A (lower) and Unit C (upper) each constitute a fining-upward sequence deposited from an individual flood event. The central Unit B, made up of alternating thin-bedded sandstone/mudstone couplets, reflects a time interval of low discharges. The flood events gave rise to channel bars, represented by large-scale inclined stratasets and correlative trough cross-bedded sandstones. Bar development in the bend and in the straight reach showed significant contrast. In the bend bank-attached lateral bars developed, whereas in the straight downstream reach mid-channel bars formed. The simple architecture of the surveyed bars suggests that they are unit bars. The bars migrated and extended downstream along the bend. In each of Units A and C, within the bend, the bars upstream partly overlapped the bars downstream, yielding incipient compound bars. Complete topset preservation in the large-scale inclined bedsets, and bar superposition, suggests rapid vertical aggradation of the river bed and points to high rates of sedimentation and transport-limited flow conditions.

The Cantacorbs channel operated under fluctuating water discharges and high sediment loads, with flood stages reaching bankfull depth. Incision depth may have been indirectly related to infilling flows through available discharges and local base level. Infilling evolved through two flood phases (related to Units A and C) separated by repeated low-water discharges spanning an unknown length of time during deposition of Unit B.

ACKNOWLEDGEMENTS

The senior author (GGB) acknowledges financial aid from the Spanish Ministry of Education to visit the University of Barcelona on several occasions and expresses his gratitude to colleagues and personnel of the University of Barcelona for their hospitality. Financial support for this work came from Project PB2002-04316-C03-01, Grup de Qualitat SRG2005-0074 de la Generalitat de Catalunya, DURSI. We thank Dr S. Georgieff (Universidad de Tucumán), anonymous journal reviewers and, in particular, Drs J. Bridge (Binghamton University) and B. Wilkinson (Syracuse University), for their helpful criticisms.

REFERENCES

Allen, P.A., Cabrera, L., Colombo, F. and **Matter, A.** (1983) Variations in fluvial style on the Eocene-Oligocene alluvial fan of the Scala Dei Group, SE Ebro Basin, Spain. *J. Geol. Soc. London*, **140,** 133–146.

Anadón, P., Cabrera, L., Colldeforms, B., Colombo, F., Cuevas, J.L. and **Marzo, M.** (1989) Alluvial fan evolution in the S.E. Ebro Basin: response to tectonics and lacustrine base level changes. In: *Excursion Guidebook, 4th International Conference on Fluvial Sedimentology* (Eds M. Marzo and C. Puigdefábregas), pp. 91. Servei Geológic de Catalunya, Barcelona.

Anadón, P., Cabrera, L., Choi, S.J., Colombo, F., Feist, M. and **Sáez, A.** (1992) Biozonación del Paleógeno continental de la zona oriental de la Cuenca del Ebro mediante carófitas: implicaciones en la biozonación general de carófitas de Europa Occidental. *Acta Geol. Hisp.*, **27,** 69–94.

Barbera, X., Cabrera, L., Marzo, M., Parés, J.M. and **Agusti, J.** (2001) A complete terrestrial Oligocene magnetostratigraphy from the Ebro Basin, Spain. *Earth Planet. Sci. Lett.*, **187,** 1–16.

Best, J.L., Ashworth, P.J., Bristow, C.S. and **Roden, J.** (2003) Three-dimensional sedimentary architecture of a large, mid-channel sand braid bar, Jamuna River, Bangladesh. *J. Sed. Res.*, **73,** 516–530.

Bridge, J. (2003) *Rivers and Floodplains: Forms, Processes, and Sedimentary Record*. Blackwell Publishing, Oxford, 491 pp.

Bridge, J. (2006) Fluvial facies models: recent developments. In: *Facies Models Revisited* (Eds H.W. Posamentier and R.G. Walker), *SEPM Spec. Publ.*, **84,** 85–170.

Bridge, J., Jalfin, G.A. and **Georgieff, J.M.** (2000) Geometry, Lithofacies, and Spatial Distribution of Cretaceous Fluvial Sandstone Bodies, San Jorge Basin, Argentina: outcrop Analog for the Hydrocarbon-Bearing Chubut Group. *J. Sed. Res.*, **70,** 341–359.

Cabrera, L.L., Colombo, F. and **Robles, S.** (1985) Sedimentation and tectonics interrelationships in the Paleogene marginal alluvial systems of the SE Ebro Basin. Transition from alluvial to shallow lacustrine environments. In: *6th European Regional IAS Meeting, Lleida, Excursion Guidebook*, **10,** 395–492.

Coleman, J.M. (1969) Brahmaputra River: channel processes and sedimentation. *Sed. Geol.*, **3,** 129–239.

Colombo, F. (1994) Normal and reverse unroofing sequences in syntectonic conglomerates as evidence of progressive basinward deformation. *Geology*, **22,** 235–238.

Cuevas, J.L., Arbués, P., Cabrera, L. and **Marzo, M.** (2007) Anatomy and architecture of ephemeral, ribbon-like channel-fill deposits of the Caspe Formation (Upper Oligocene to Lower Miocene of the Ebro Basin, Spain). In: *Sedimentary Processes, Environments and Basins: A Tribute to Peter Friend* (Eds G. Nichols, E. Williams and C. Paola), *IAS Spec. Publ.*, **38,** 591–611.

Friend, P.F., Slater, M.J. and **Williams, R.C.** (1979) Vertical and lateral building of ribbon sandstone bodies, Ebro Basin, Spain. *J. Geol. Soc. London*, **136,** 39–46.

Gibling, M.R. and **Rust, B.R.** (2006) Ribbon sandstones in the Pennsylvanian Waddens Cove Formation, Sydney Basin, Atlantic Canada: the influence of siliceous duricrusts on channel-body geometry. *Sedimentology*, **37,** 45–66.

Haszeldine, R.S. (1983) Fluvial bars reconstructed from a deep straight channel, Upper Carboniferous Coalfield of NE England. *Sedimentology*, **31,** 811–822.

King, M.R. (2008) *Fluvial architecture of the interval spanning the Pittsburgh and Fishpot limestones (Late Pennsylvanian), southeastern Ohio*. Master of Science thesis (unpublished), The College of Arts and Sciences of Ohio University, 134 pp.

Luppi, L., Rinaldi, M., Teruggi, L.B., Darby, S.E. and **Nardi, L.** (2009) Monitoring and numerical modelling of riverbank erosion processes: a case study along the Cecina River (central Italy). *Earth Surf. Proc. Land.*, **34,** 530–546.

Möhrig, D., Heller, P.L., Paola, C. and **Lyons, W.J.** (2000) Interpreting avulsion process from ancient alluvial sequences: Guadalope-Matarranya system (northern Spain) and Wasatch Formation (western Colorado). *Geol. Soc. Am. Bull.*, **112,** 1787–1803.

Nichols, G. (2007) Fluvial systems in desiccating endorheic basins. In: *Sedimentary Processes, Environments and Basins: A Tribute to Peter Friend* (Eds G. Nichols, E. Williams and C. Paola), *IAS Spec. Publ.*, **38,** 569–589.

Reesink, A.J.H. and **Bridge, J.S.** (2007) Influence of superimposed bedforms and flow unsteadiness on formation of cross strata in dunes and unit bars. *Sed. Geol.*, **202,** 281–296.

Riba, O., Villena, J. and **Quirantes, J.** (1967) Nota preliminar sobre la sedimentación en paleocanales terciarios de la zona de Caspe-Chipriana (Provincia de Zaragoza). *Anal. Edafol. y Agrobiol.*, **26,** 617–634.

Sambrook Smith, G.H., Ashworth, P.J., Best, J.L., Woodward, J. and **Simpson, C.J.** (2006) The sedimentology and alluvial architecture of the sandy braided South Saskatchewan River, Canada. *Sedimentology*, **53,** 413–434.

Santanach, P. (1997) The Ebro Basin in the structural framework of the Iberian Plate. In: *Sedimentary Deposition in Rift and Foreland Basins in France and Spain* (Eds G. Busson and B. de Screiber), pp. 303–318. Columbia University Press, New York.

Sheets, B.A., Paola, C. and **Kelberer, J.M.** (2007) Creation and preservation of channel-form sand bodies in an experimental alluvial system. In: *Sedimentary Processes, Environments and Basins: A Tribute to Peter Friend* (Eds G. Nichols, E. Williams and C. Paola), *IAS Spec. Publ.*, **38,** 555–567.

Smith, N.D. (1971) Transverse bars and braiding in the lower Platte River, Nebraska. *Geol. Soc. Am. Bull.*, **82,** 3407–3420.

Smith, R.M.H. (1995) Changing fluvial environments across the Permian-Triassic boundary in the Karoo Basin, South Africa and possible causes of tetrapod extinctions. *Palaeogeogr. Palaeoclimatol. Palaeoecol.*, **117,** 81–104.

Stear, W.M. (1983) Morphological characteristics of ephemeral stream channel and overbank splay sandstone bodies in the Permian Lower Beaufort Group, Karoo Basin, South Africa. *IAS Spec. Publ.*, **6,** 405–420.

Swanson-Hysell, N. (2005) *Magnetic Reversal Stratigraphy in the Ebro Basin, near Horta de Sant Joan, Spain*. BA thesis (unpublished), Carleton College, Northfield, MN, 39 pp.

Tubino, M. (1991) Growth of alternate bars in unsteady flows. *Water Resour. Res.*, **27,** 37–52.

Villena, J., González, A., Muñoz, A., Pardo, G. and **Pérez, A.** (1992) Síntesis estratigráfica del Terciario del borde Sur de la Cuenca del Ebro: unidades genéticas. *Acta Geol. Hisp.*, **27,** 225–245.

Wan, Z. (1985) Bed material movement in hyperconcentrated flow. *J. Hydraul. Eng.*, **111,** 87–1002.

Williams, R.C. (1975) *Fluvial deposits of Oligo-Miocene age in the southern Ebro Basin. Spain*. PhD thesis (unpublished), University of Cambridge, 221 pp.

Wilson, I.G. (1973) Equilibrium cross-section of meandering and braided rivers. *Nature*, **241,** 393–394.

Manuscript received 23 November 2008; revision accepted 22 October 2009